Available online at www.sciencedirect.com

ScienceDirect

Procedia CIRP 94 (2020) 505–510

www.elsevier.com/locate/procedia

11th CIRP Conference on Photonic Technologies [LANE 2020] on September 7-10, 2020

Multi objective optimization of water jet guided laser micro drilling on Inconel 718 using Taguchi Method

Levent Subasi[a,b]*, Mustafa I. Gokler[b], Ulas Yaman[b]

[a]*TUSAS Engine Industries Inc., 26210, Eskisehir, Turkey*
[b]*Middle East Technical University, 06800, Ankara, Turkey*

* Corresponding author. Tel.: +90-222-211-2100. *E-mail address:* levent.subasi@tei.com.tr

Abstract

Water jet guided laser overcomes the adverse effects of conventional laser cutting and drilling processes, such as heat-affected-zone, spatter, burr formation, etc. Pressurized water in this novel process provides focusing, cooling and cleaning on the cut region, eliminating undesired side effects of the laser. The process is nowadays used in energy and aerospace industries for drilling micro cooling holes on turbine blades made of super alloys. However, more research on the process is required to understand the effects of the variables on cutting time and quality. Optimum conditions differ for various materials and geometries. In this study, a multi objective optimization is performed in terms of process time and taper of the micro holes drilled on Inconel 718, a commonly used material in gas turbines. Taguchi design of experiment and statistical analysis is used to perform the experiments and evaluate the results.

Keywords: Laser drilling; Inconel718; Optimization; Taguchi

1. Introduction

Laser drilling is a widely used manufacturing technology in aerospace industry [1]. The process is especially useful for drilling micro cooling holes on turbine blades, which is of critical importance in order for the parts to withstand high temperatures in the gas turbine. However, although considered as a fast process, lasers have some quality issues associated with high heat input to the material [2].

Various optimization and modeling studies have been done to overcome these issues on different materials and with different kinds of laser systems. Chatterjee et al. [3] investigated the quality characteristics in Nd:YAG laser drilling of stainless steel using Taguchi method. They have found a relation between laser parameters, heat affected zone (*HAZ*), and spatter area formation. Wang et al. [4] focused on hole roundness, taper and recast layer in drilling cooling holes on a super alloy. They have found out that spiral tool path should be used for better results. Su et al. [5] performed fiber laser drilling optimization on a ceramic material. They have found out the optimal peak power and ablation time for the best hole characteristics, such as diameter, circularity, taper and recast layer. Parthiban et al. [6] optimized the parameters for Nd:YAG laser micro-drilling process of a Nickel based super alloy with thermal barrier coating (*TBC*) using a galvo scanner. Taguchi orthogonal array was used for conducting the experiments. Surface roughness and surface crack density were the measured outputs. Optimum inclination angle, scan speed and number of passes were determined in return.

Water jet guided laser technology, which was developed by the Swiss company Synova S.A. in late 1990s as an innovative approach, has become an alternative to the dry lasers. The laser beams are guided within a water-jet, so that focusing, cooling and cleaning effects of the water are benefited from (see Fig. 1). The technology is used for various applications in different industries. Although its success is demonstrated

10.1016/j.procir.2020.09.172

many times compared to the dry lasers in terms of quality (heat affected zone, recast layer, spatter, burr formation, etc.), the technology is still not widely elaborated. It is very difficult to model the process due to constantly flowing pressurized water splashing back from the surface. There are many variables in the process, which affects the material removal rates and quality of the cuts.

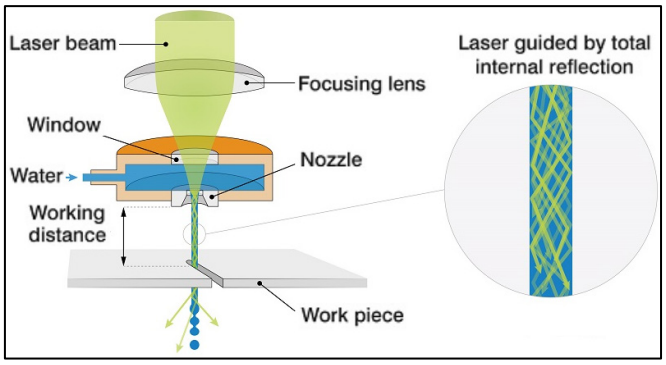

Fig. 1. Working principle of the water jet guided laser [7].

In this paper, the main aim is to perform a multi objective optimization in terms of process time and taper angle of the micro holes drilled on Inconel 718 super alloy using water jet guided laser. Taguchi method and Overall Evaluation Criteria (*OEC*) are used for this purpose. In the following sections, the related independent variables effecting the outputs and the experimental methods are presented and the results are discussed.

2. Materials and Methods

2.1. Material

Solution and Precipitation Heat Treated Wrought Inconel 718 material was used in the experiments. Nominal composition of the material is given in Table 1 per the specification SAE AMS 5663N and some of the material properties at room temperature are provided in Table 2.

2.2. Sample

A specimen with dimensions of 20 × 20 × 5.6 mm was cut from a bulk material using Electrical Discharge Machining (*EDM*) method. The thickness was intentionally chosen as 5.6 mm, so that when cooling holes of diameter 0.4 mm were drilled, it would yield to an aspect ratio of 14:1, which is a design criterion. The surface area is large enough to perform repetitive tests.

2.3. Machine

The machine utilizes a diode pumped and pulsed Nd:YAG laser with 532 nm wavelength. The laser beam is carried to the nozzle with a 150 µm fiber. The water used in the machine for the water jet is purified by reverse osmosis method to achieve a resistivity level of 17 MΩcm. In order to stabilize the water jet, Helium is used as an assisting gas.

Table 1. Nominal composition of Inconel 718.

Al	C	Co	Cr	Cu	Fe	Mn	Mo	Nb	Ni	Si	Ti
0.5	0.08	1	19	0.3	16.7	0.35	3.1	5.2	52.5	0.35	0.9

Table 2. Material Properties of Inconel 718 [8].

Property	Unit	Value
Hardness	HB	331
Yield Strength at 0.2% Offset	MPa	1034
Ultimate Tensile Strength	MPa	1241
Density	kg m^{-3}	8190
Melting Temperature	°C	1260
Heat Capacity	J K^{-1} g^{-1}	0.435

2.4. Cutting method

Since the laser beam can focus on a small spot, which is as wide as the water jet diameter, it is possible to apply different tool path strategies for drilling micro holes. This is different than the conventional methods used, such as percussion or trepanning drilling. The hole drilling process was completed in two steps. First, the hole was pierced with spiral drilling technique, and then another finishing tool path was used as shown in Fig. 2. The reason for employing the finishing step is to obtain the required diameter at the exit side of the hole. These tool paths can be parametrically adjusted by defining the spiral diameter and the size of the spiral step. The laser beam moves in X-axis, whereas the sample moves in Y-axis for this setup.

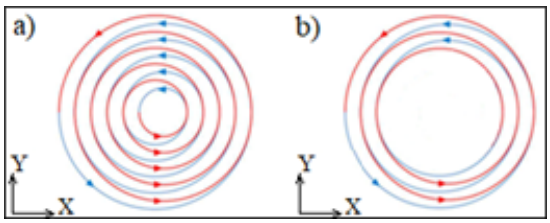

Fig. 2. (a) first step; (b) second step.

2.5. Hole geometry

Diameter of the holes to be drilled were 0.4 mm. The total depth was 5.6 mm, corresponding to an aspect ratio of 14:1. The holes were drilled perpendicular to the workpiece surface.

2.6. Process window

For the experiments, five different factors were considered, namely laser power, pulse width, frequency, feed and spiral step. The minimum and maximum levels of these factors chosen for the experiments depend on the machine constraints and previous experiences.

Among variety of nozzles, 50 µm sapphire nozzle was selected for the experiments since it performed well during the screening tests. Water jet pressure and gas flow were set to 200 bar and 1 l/min, respectively. They were kept constant during the trials. Similarly, the standoff distance from the nozzle to the sample surface was kept constant at 10 mm.

2.7. Experiments

The factors and levels are shown in Table 3. Since there are 5 factors and two kinds of mixed levels, a modified Taguchi L-16 orthogonal table is used for the experiments [9]. The factors and levels for each trial are shown in Table 4.

Table 3. Factors and levels.

Factors	Level 1	Level 2	Level 3	Level 4
A. Laser Power (W)	25	30	35	–
B. Pulse Width (ns)	200	250	300	–
C. Frequency (kHz)	10	15	20	–
D. Feed (mm/min)	60	120	180	240
E. Spiral Step (mm)	0.010	0.015	0.020	0.025

Table 4. Modified Taguchi L-16 orthogonal table.

Trial	A.	B.	C.	D.	E.
1	25	200	10	60	0.010
2	25	250	15	120	0.015
3	25	300	20	180	0.020
4	25	250	15	240	0.025
5	30	200	15	180	0.025
6	30	250	10	240	0.020
7	30	300	15	60	0.015
8	30	250	20	120	0.010
9	35	200	20	240	0.015
10	35	250	15	180	0.010
11	35	300	10	120	0.025
12	35	250	15	60	0.020
13	30	200	15	120	0.020
14	30	250	20	60	0.025
15	30	300	15	240	0.010
16	30	250	10	180	0.015

In order to increase the reliability of the analysis, every trial was repeated three times. Therefore, 48 holes were drilled in total. The objective of the experiments was to decrease the process time and the taper of the holes.

2.8. Measurement

The process time was measured with a chronometer. Diameters of the holes were measured with a steel pin gage set, which has 0.01 mm increments. Then, the taper angle (T_a) was calculated as follows

$$T_a = tan^{-1}\left(\frac{D_t - D_b}{2t}\right) \quad (1)$$

where, D_t is the diameter at the entrance (top), D_b is the diameter at the exit (bottom), and t is the hole depth (workpiece thickness), which is always 5.6 mm in these experiments.

3. Results and Discussion

Analysis is performed using Signal-to-Noise ratio (*S/N*) proposed by Taguchi [9]. *S/N* ratio is a variance index dependent on mean square deviation (*MSD*). The advantage of using *S/N* value is that it both contains the mean value and the variance of the data considered. The equation of *S/N* is

$$S/N = -10\,log_{10}(MSD) \quad (2)$$

The value of *MSD* in this equation, depends on the quality characteristic, whether it is “smaller is better”, “nominal is better” or “larger is better”. Considering process time and taper angle, they both fit with the “smaller is better” case, for which the equation is given as

$$MSD = (y_1^2 + y_2^2 + y_3^2 + \cdots)/n \quad (3)$$

where, y_i’s are the obtained results for each repeated test and n is the number of repetitions, which is always 3 in this study.

The drilled specimen is shown in Fig. 3. The mean value and *S/N* values of the process time and taper angle of the holes obtained after the trials are given in Table 5.

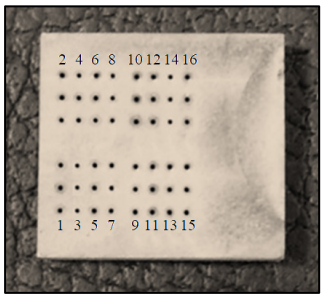

Fig. 3. Drilled specimen.

Table 5. Results of the experiments.

	Process Time		Taper Angle	
Trial	Mean (s)	*S/N*	Mean (°)	*S/N*
1	361	–51.162	0.46	6.702
2	914	–59.217	0.49	6.106
3	2917	–69.300	0.53	5.569
4	1249	–61.936	0.53	5.528
5	668	–56.497	0.60	4.476
6	305	–49.773	0.46	6.702
7	880	–58.896	0.65	3.763
8	2390	–67.576	0.56	4.970
9	776	–57.814	0.55	5.203
10	312	–49.940	0.43	7.310
11	163	–44.262	0.34	9.322
12	285	–49.101	0.43	7.392
13	539	–54.640	0.38	8.498
14	2008	–66.058	0.41	7.760
15	821	–58.339	0.55	5.253
16	192	–45.666	0.36	8.861
Average	924	–56.261	0.48	6.463

The response plots with the mean values are given in Fig. 4 and Fig 5.

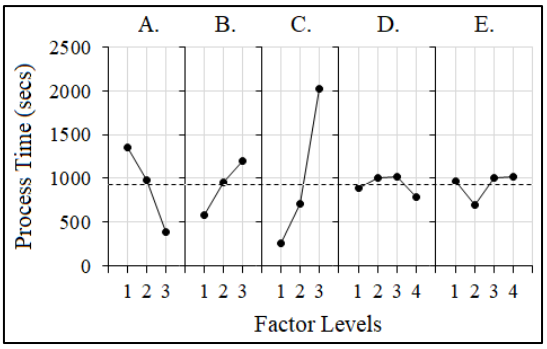

Fig. 4. Response plots for process time.

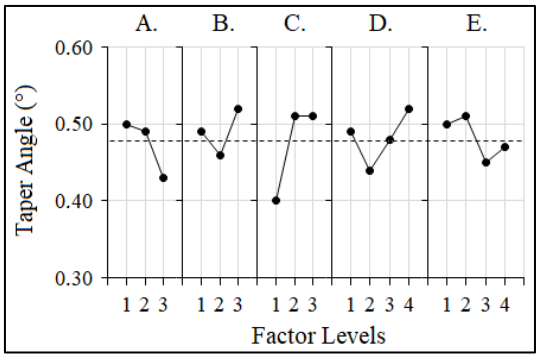

Fig. 5. Response plots for taper angle.

Tables of the main effects for process time and taper angle are provided in Table 6 and Table 7. When considering *S/N* values, larger value always indicates a better result. Thus, considering the values in the tables, laser power should be chosen as 35 W and frequency as 10 kHz for the optimal condition. However, there are conflicts with the optimum pulse width, feed and spiral step values.

Table 6. Main (average) effects of factors for process time in terms of *S/N*.

	Average Effects			
Factors	Level 1	Level 2	Level 3	Level 4
A. Laser Power (W)	–60.404	–57.181	–50.279	–
B. Pulse Width (ns)	–55.028	–56.159	–57.699	–
C. Frequency (kHz)	–47.716	–56.071	–65.187	–
D. Feed (mm/min)	–56.304	–56.424	–55.351	–56.966
E. Spiral Step (mm)	–56.754	–55.398	–55.703	–57.188

Table 7. Main (average) effects of factors for taper angle in terms of *S/N*.

	Average Effects			
Factors	Level 1	Level 2	Level 3	Level 4
A. Laser Power (W)	5.976	6.286	7.307	–
B. Pulse Width (ns)	6.220	6.829	5.977	–
C. Frequency (kHz)	7.897	6.041	5.876	–
D. Feed (mm/min)	6.404	7.224	6.554	5.671
E. Spiral Step (mm)	6.059	5.983	7.040	6.772

3.1. OEC analysis

It is not always possible to find the same optimum factor levels for every characteristic at the same time. In these circumstances, the relative weight of each characteristic can be combined into one *OEC* index. It is then possible to perform optimization based on these new values [9].

In order to calculate the *OEC*, which is a dimensionless index between 0 and 1, one needs to determine the weight of each characteristic, the best and worst readings of the experiments. Then, the *OEC* can be defined as

$$OEC = \frac{y_{1max} - y_1}{y_{1max} - y_{1min}} \times w_1 + \frac{y_{2max} - y_2}{y_{2max} - y_{2min}} \times w_2 + \cdots \quad (4)$$

where, y_i is the measured reading, y_{imax} and y_{imin} is the worst and best readings of each characteristic for "smaller is better" case and w_i is the weight of each characteristic. The weights are determined based on the importance of the characteristics for the practitioner. Assuming taper angle (quality) is more important than process time, the related values for calculating *OEC* are given in Table 8.

Table 8. *OEC* description.

Criteria Description	Best Reading	Worst Reading	Relative Weight
1. Process Time (s)	161	2975	40%
2. Taper Angle (°)	0.31	0.67	60%

The mean and *S/N* values of the combined *OEC* index of process time and taper angle are given in Table 9. The main effects table of *OEC* is given in Table 10. The *MSD* value in order to find the *S/N* ratio is calculated according to "larger is better" case, for which the equation is given as

$$MSD = (1/y_1^2 + 1/y_2^2 + 1/y_3^2 + \cdots)/n \quad (5)$$

Table 9. *OEC* scores.

	Values of each repetition					
Trial	*OEC*#1	*OEC*#2	*OEC*#3	Mean	*MSD*	*S/N*
1	0.80	0.63	0.71	0.71	2.013	–3.038
2	0.64	0.55	0.55	0.58	3.032	–4.817
3	0.23	0.26	0.23	0.24	17.598	–12.455
4	0.51	0.49	0.42	0.47	4.552	–6.582
5	0.41	0.42	0.50	0.44	5.230	–7.185
6	0.63	0.81	0.73	0.72	1.978	–2.961
7	0.29	0.30	0.39	0.33	9.869	–9.943
8	0.26	0.18	0.32	0.25	18.170	–12.594
9	0.39	0.66	0.49	0.51	4.341	–6.376
10	0.80	0.90	0.64	0.78	1.754	–2.440
11	0.91	1.00	0.91	0.94	1.132	–0.537
12	0.81	0.81	0.73	0.78	1.647	–2.166
13	0.77	0.86	0.86	0.83	1.457	–1.634
14	0.56	0.58	0.56	0.57	3.123	–4.946
15	0.55	0.48	0.49	0.51	3.939	–5.954
16	1.00	0.91	0.82	0.91	1.230	–0.898

Table 10. Main (average) effects of factors for *OEC* in terms of *S/N*.

	Average Effects			
Factors	Level 1	Level 2	Level 3	Level 4
A. Laser Power (W)	–6.723	–5.764	–2.880	–
B. Pulse Width (ns)	–4.558	–4.675	–7.222	–
C. Frequency (kHz)	–1.858	–5.090	–9.092	–
D. Feed (mm/min)	–5.023	–4.895	–5.744	–5.468
E. Spiral Step (mm)	–6.006	–5.508	–4.804	–4.813

When considering *OEC* values, larger value always indicates a better result. Thus, looking at the table, laser power should be chosen as 35 W, pulse width as 200 ns, frequency as 10 kHz, feed as 120 mm/min and spiral step as 0.020 mm for the optimal condition ($A_3B_1C_1D_2E_3$). These factor levels should allow a less tapered hole to be processed with minimal process time.

3.2. Analysis of variance (ANOVA)

ANOVA analysis is also performed to see the significance levels of all the factors. The *ANOVA* table for *OEC* mean values can be seen in Table 11. Looking at the percentage values in the table, frequency is the most dominant factor affecting the results. Feed and spiral step are less important, even statistically insignificant factors, so it is up to the practitioner to choose their levels arbitrarily.

Table 11. *ANOVA* analysis.

Factors	DOF (f)	S	V	F	S'	P (%)
A. Laser Power (W)	2	0.141	0.070	16.372	0.132	17.8
B. Pulse Width (ns)	2	0.048	0.024	5.637	0.040	5.4
C. Frequency (kHz)	2	0.369	0.185	42.996	0.361	48.6
D. Feed (mm/min)	3	0.015	0.005	1.134	0.002	0.2
E. Spiral Step (mm)	3	0.020	0.007	1.519	0.007	0.9
Other/Error	35	0.150	0.004	–	–	27.2
Total	47	0.743	–	–	–	100.0

3.3. Estimation of performance

It is also possible to calculate the expected outputs based on the selected factor levels at this point. Contribution of each factor level on the average value is taken into consideration one by one for each characteristic, as shown in Table 12.

Table 12. Estimation of performance for the optimal condition.

	Process Time			Taper Angle		
Factors	Average	*S/N* Opt	Contribution	Average	*S/N* Opt	Contribution
A.	–56.261	–50.279	5.981	6.463	7.307	0.847
B.	–56.261	–55.028	1.232	6.463	6.220	–0.240
C.	–56.261	–47.716	8.545	6.463	7.897	1.437
D.	–56.261	–56.424	–0.163	6.463	7.224	0.764
E.	–56.261	–55.703	0.558	6.463	7.040	0.580
Total			16.155			3.388
Est.		–40.106			9.848	

The estimated *S/N* value is calculated by adding the total contribution to the average performance, which is -56.261 for process time and 6.463 for taper angle. Based on the estimated *S/N* values, the expected values for process time and taper angle can be found by the equation provided below.

$$MSD = \sigma^2 + (y_a - y_0)^2 \quad (6)$$

where, σ is the standard deviation, y_a is the sample average and y_0 is the target value. Considering the average value only and "smaller is better" case, $\sigma=0$ and $y_0=0$. Then, using Equation (2) and simplifying, Equation (6) becomes:

$$y_a = \sqrt{10^{-\frac{S/N}{10}}} \quad (7)$$

Therefore, using Equation (7) and the estimated *S/N* values in Table 12, the process time is calculated as 101 s and taper angle as 0.32° at the optimum condition.

3.4. Verification tests

In order to verify the estimated performance, verification tests with 5 repeats are performed. Using the optimal condition ($A_3B_1C_1D_2E_3$), the mean values of the obtained results are close to the expected values, as shown in Table 13.

Table 13. Confirming predicted results.

Criteria Description	Expected Reading	Verification Result
1. Process Time (s)	101	120
2. Taper Angle (°)	0.32	0.24

The reason for errors or deviations between the expected and the verified results are related to the confidence interval of the estimated performance. Since there are other factors affecting the process, such as real-life disturbances, variations and/or interactions between factors, deviations are always expected. In this case, the results seem close. Average taper angle performance of 0.24° is even better than expected, which is a value that couldn't be obtained in the initial trials.

3.5. Peak Intensity

Since the power of the laser source is transmitted to the work piece through a fiber and water jet, a transmission loss should be taken into account. Experiments with the system show that the ratio is approximately 0.75. The pulse energy E_p (mJ) can be calculated as in [10] below.

$$E_p = 0.75P/f \quad (8)$$

where, P (W) is the average laser power and f (kHz) is the frequency. Then, the peak power P_p (kW) can be calculated as

$$P_p = E_p/\tau_p \quad (9)$$

where, τ_p (ns) is the pulse width. Finally, the power density or peak intensity I_p (GW/cm^2) can be calculated by using the below equation.

$$I_p = P_p / A \quad (10)$$

where, A (cm^2) is the water jet cross-section area. The area is calculated by taking the diameter (µm) of the nozzle and multiplying it by a contraction factor, which shows the ratio of the water jet diameter compared to the nozzle diameter. Experiments with the system show that this factor is approximately 0.83.

Then, using Equations (8), (9), (10), taking the nozzle diameter as 50 µm, using the related factors and the unit conversions, below equation is obtained.

$$I_p = \frac{55.475P}{f\tau_p} \quad (11)$$

Peak intensity is a compact value including all of the laser parameters used in the experiments. Calculating the peak intensity, and matching against the process time measured in the experiments, the plot shown in Fig. 6 can be obtained. It is clear that there is a strong dependence between the two variables.

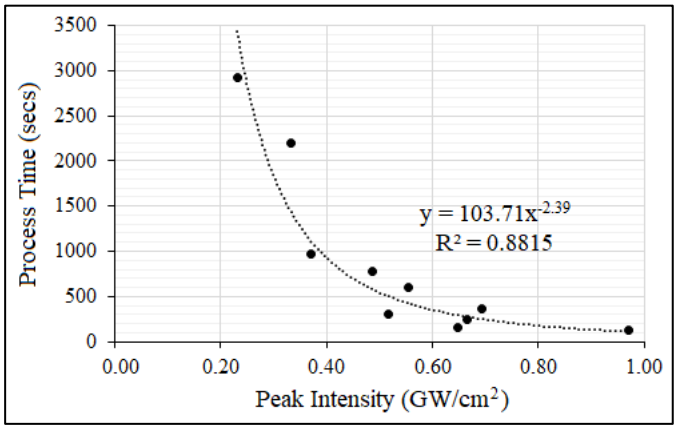

Fig. 6. Peak intensity vs. Process time plot.

Thus, it is justified that the optimum condition of 35 W, 200 ns and 10 kHz provides better processing time since their calculated peak intensity of 0.97 is higher compared to the values used at initial trials.

Considering Equation (11), it seems possible to increase the peak intensity even more, in order to decrease the process time. Laser power should be increased and/or frequency and pulse width should be decreased for this purpose. However, the power density is a constraint for the machine. The damage threshold of the water jet nozzle is approximately 1 GW/cm^2. This limit should not be exceeded and the optimum condition is already very close to the limit. Thus, there is not much room for further improvement.

4. Conclusion

A multi objective optimization is performed in terms of process time and taper angle of the micro holes drilled on Inconel 718 material using water jet guided laser. Taguchi design of experiment, *S/N* analysis, *OEC* analysis and *ANOVA* analysis were used for evaluation of results and optimization.

Taguchi approach is proved to be useful, as also verified by further tests. Both process time and taper angle objectives are optimized by adjusting the levels. Frequency is the key factor when both objectives are considered.

Other non-laser factors, such as feed and spiral step are insignificant. In fact, these two factors only control how much the laser beam is overlapping on the surface. More overlap means faster material removal in Z (hole depth) direction, whereas less overlap means faster material removal in XY plane. It turns out that the total process time is not highly affected by changing these values, so the total material removal rate is directly correlated with the laser parameters.

Faster process time is obtained by using the laser parameters that yields to higher peak intensity. Thus, for better performance laser power should be increased or pulse width and frequency should be decreased, taking into account the damage threshold of the nozzle.

The design of experiment did not include any possible interactions or noise factors. Looking at the *ANOVA* table, the error term percentage of 27.2% suggests that there might be some other effects, such as power and pulse width fluctuations, or water splash back blocking the laser beam. As a future work, further experiments shall be performed to understand the factor interactions and fine-tune the results even more. It is also possible to expand the process window to include different factor levels or experiment with different factors, such as nozzle diameter, water and gas pressure, etc.

Acknowledgements

The authors would like to thank to Ronan Martin (Synova SA) and Jérémie Diboine (Synova SA) for their support.

References

[1] Darwish SMH, Ahmed N, Al-Ahmari AM. Laser Beam Micro-milling of Micro-channels in Aerospace Alloys. Singapore: Springer; 2017.
[2] Gautam GD, Pandey AK. Pulsed Nd:YAG laser beam drilling: A review. Optics and Laser Technology; 2018; 100, p. 183-215.
[3] Chatterjee S, Mahapatra SS, Sahu AK, Bhardwaj VK, Choubey A, Upadhyay BN, Bindra KS. Experimental Investigation Of Quality Characteristics In Nd:YAG Laser Drilling Of Stainless Steel (AISI 316). Materials Today; 2018; 5, p. 11526–11530.
[4] Wang M, Yang L, Zhang S, Wang Y. Experimental investigation on the spiral trepanning of K24 superalloy with femtosecond laser. Optics and Laser Technology; 2018; 101, p. 284-290.
[5] Su L, Chen R, Huang Z, Zhou M, Zeng Q, Shi Q, Liao Z, Lu T. Geometrical morphology optimisation of laser drilling in B4C ceramic: From plate to hollow microsphere. Ceramics International; 2018; 44, p. 1370-1375
[6] Pathiban K, Duraiselvam M, Manivannan R. TOPSIS based parametric optimization of laser micro-drilling of TBC coated nickel based superalloy. Optics and Laser Technology; 2018; 102, p. 32-39.
[7] www.synova.ch/technology/laser-microjet.html (last accessed 20.02.2020)
[8] Mills KC. Recommended values of thermophysical properties for selected commercial alloys. Cambridge: Woodhead Publishing; 2002.
[9] Roy RK. A Primer on the Taguchi Method. 2nd ed. Michigan: Society of Manufacturing Engineers; 2010.
[10] Yeo CY, Tam SC, Jana S, Lau MWS. A technical review of the laser drilling of aerospace materials. Journal of Materials Processing Technology; 1994; 42, p. 15-49.